Photoinduced Initiation of Olefin Polymerization: Enabling Spatial Control with Light

Jordan M. Kaiser,[‡] Justin M. Burroughs,[‡] and Brian K. Long*

Department of Chemistry, University of Tennessee, Knoxville, Tennessee 37996-1600, United States

ABSTRACT: Polyolefins constitute the majority of plastics produced worldwide. Despite the variety of precatalyst activation mechanisms known in literature, the development of spatially controlled olefin polymerizations remains relatively unknown. If successful, control over the olefin polymerization process could provide unprecedented synthetic control and potentially broaden industrial applications. Herein, we demonstrate a simple olefin polymerization methodology termed photoinduced initiation of olefin polymerization (PIOP), wherein photoacid generators are used in conjunction with controlled irradiation to achieve precatalyst activation and olefin polymerization. These results demonstrate that PIOP can be used for solution-based polymerizations of ethylene and α-olefins, and may be extended to heterogeneous polymerizations of gaseous ethylene and propylene, thereby achieving spatial control over the olefin polymerization process.

Introduction

Polyolefins are the most abundantly produced and widely used polymers in modern society, recently reaching over 184 million tons worldwide in 2017.[1] These materials continue to garner tremendous industrial interest as they are derived from inexpensive monomer feedstocks and have tailorable thermal and mechanical properties. Since their discovery, tremendous efforts have been devoted to development of cost-effective, efficient, and highly selective olefin polymerization catalyst systems, which is primarily accomplished through the design of new, and often complex, ligand scaffolds.[2-12] The vast majority of these homogeneous, transition metal-based olefin polymerization precatalysts must be activated prior to polymerization via the addition of an activator or co-catalyst. These precatalyst activation methods include: alkyl/halide abstraction by neutral Lewis acids or charged reagents, one electron oxidation or reduction, halide/alkyl exchange followed by alkyl abstraction, and protonolysis of metal-alkyl bonds by Brønsted acids.[13]

In contrast, very few research reports have appeared in recent literature detailing new activation methods that may impart enhanced control over the polymerization process. For example, though currently employed olefin polymerization precatalyst activation methods may achieve temporal control over the precatalyst initiation event through timed injection of co-catalyst, spatial control has yet to be demonstrated. Motivated by inability to exert spatial control over the olefin polymerization process, we considered the use of latent catalysis, a field of research that has recently emerged as a powerful tool within the field of polymer synthesis.[14-17]

Many examples of latent catalysis employ external stimuli to access active/dormant catalytic species, on demand.[18-23] Of the commonly used external stimuli, light is frequently employed due to its readily available and non-invasive nature, as well as its ability to deliver both temporal and spatial resolution. Indeed, light has been used as an effective stimulus to simultaneously enable temporal and spatial control for polymerization methods such as, ring opening metathesis polymerization (ROMP), cationic polymerization, radical polymerization, metal–organic insertion light initiated radical (MILRad),[24, 25] and photocuring of resins, all without the need to inject additional reagents or perturb reaction parameters. [14, 15, 26]These polymerization methods have been exploited in a variety of applications that include photolithography, macroscopic/microscopic patterning, and even advanced 3-D printing techniques such as dynamic light processing and stereolithography.[27-32] Unfortunately, however, the use of light as a stimulus to control the coordination-insertion polymerization of olefins has been limited to the photoreduction of heterogeneous titania and Cr/SiO_2 catalyst systems,[33, 34] while spatiotemporal control of homogeneous coordination-insertion olefin polymerization has heretofore been unrealized.

Inspired by the use of Brønsted acidic olefin polymerization precatalyst activators, such as anilinium tetrakis(penta-fluorophenyl)borate (**AB**),[13] we anticipated that photoacid generators (PAGs) might serve as latent and light responsive precatalyst activator surrogates (Figure 1). More specifically, we hypothesized that irradiating of a reaction mixture containing a PAG, a dialkyl substituted olefin polymerization precatalyst, and an olefinic monomer with light of an appropriate wavelength would generate protons, in situ, via PAG photolysis[16, 35] thereby inducing precatalyst activation via protonolysis of a precatalyst metal-alkyl bond, ultimately initiating the olefin polymerization process. We envisioned that this photoinduced initiation of olefin polymerization (**PIOP**) methodology would provide a catalytic system that is dormant in the absence of light, but that spatial control over

the olefin polymerization initiation process may be realized upon controlled light exposure (Figure 1).

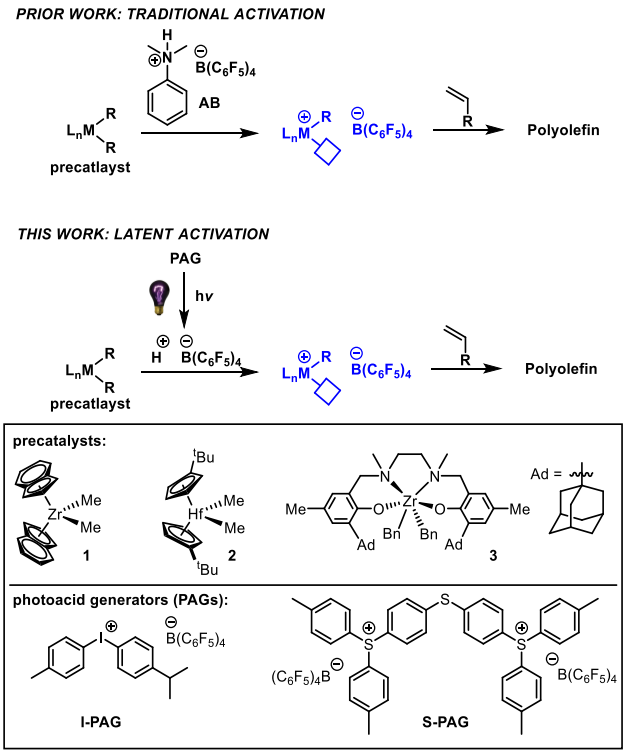

Figure 1. Polymerization of olefinic monomers using precatalysts **1**-**3** activated via a traditional Brønsted acidic activator (**AB**), or latent activation by either an iodonium (**I-PAG**) or sulfonium PAG **(S-PAG**) upon UV light irradiation.

Table 1. Photoinduced initiation of 1-hexene polymerization using precatalyst **1** and salient controls.[a]

entry	precatalyst	activator	exposure time (min)[b]	polymer yield (%)	M_w[c] (kg/mol)	$Đ$[c]
1	**1**	**I-PAG**	15	64 ± 2.3	19.7	2.6
2	**1**	**S-PAG**	15	40 ± 6.1	21.0	1.6
3[d]	**1**	**AB**	0	61 ± 1.7	25.3	1.8
4[e]	**1**	-	15	0	-	-
5[f]	-	**I-PAG**	15	0	-	-
6[f]	-	**S-PAG**	15	0	-	-
7[g]	**1**	**I-PAG**	0	0	-	-
8[g]	**1**	**S-PAG**	0	0	-	-

[a]Polymerization conditions: precatalyst **1** (10.0 μmol), PAG (10.0 μmol), 3 mL of 1-hexene, 1 mL of DCM, 20 °C, t_{rxn} = 3 h. [b]Irradiated using a handheld 4 W compact UV lamp operating at 254 nm. [c]Determined using triple detection GPC at 150 °C in 1,2,4-trichlorobenzene. [d]**AB** (10 μmol) is used instead of PAG . [e]No PAG added. [f]No precatalyst **1** is added. [g]No light exposure.

Results and Discussion

To test this hypothesis, we chose to examine the commonly used and commercially available iodonium- and sulfonium-based PAGs, 4-isopropyl-4'-methyldiphenyliodonium tetrakis(penta-fluorophenyl) borate (**I-PAG**) and bis[4-(dimethylphenyl-sulfonio)phenyl]sulfonium tetrakis(pentafluorophenyl) borate (**S-PAG**), respectively. A key selection criterion for these PAGs is the presence of weakly coordinating counterions (e.g. the $^{-}B(C_6F_5)_4$ anion), which have been vetted to be compatible with myriad olefin polymerization catalysts.[13] In regards to the precatalysts employed, they should be dialkyl substituted so as to enable activation via metal-alkyl bond protonolysis. Therefore, we chose to evaluate three common dialkyl-substituted precatalysts, which include dimethylbis(indenyl) zirconium (**1**), dimethylbis(*t*-butylcyclo-pentadinyl) hafnium (**2**), and a post metallocene ONNO-type Zr-based precatalyst (**3**)[36] for the polymerization of olefinic monomers.

Prior to polymerization studies, and as a proof-of-principle, we sought to confirm the efficacy of PAGs to activate a dialkyl-substituted olefin polymerization precatalyst upon PAG photolysis. Therein, irradiation of a reaction mixture containing a PAG (in this case **I-PAG**) and precatalyst **1** should induce protonolysis of a Zr-CH_3, which is known to occur during activation with the Brønsted acidic activator **AB**.[37] This reduction in Zr-CH_3 content can be observed using ^{1}H NMR spectroscopy wherein the integration of the Zr-CH_3 proton signal, relative to those of

an internal standard, is monitored as a function of UV light irradiation time (Figure S3). As anticipated, irradiation of a mixture of **I-PAG** and precatalyst **1** using a 254 nm light source resulted in a decrease in integrated intensity of the Zr-CH_3 signal as a function of irradiation time, suggesting activation of the precatalyst via protonolysis of the Zr-CH_3 bond and generation of an open coordination site that is required for monomer coordination and olefin polymerization. However, it was also noted that upon extended irradiation times (i.e those extending beyond 15 min, under these reaction conditions) the Zr-CH_3 integration decreases below an expected integration in which only one of the two M-alkyl substituents is cleaved. Though this observation could suggest protonolysis of more than one methyl group for some metal centers, we believe it may be due to homolytic cleavage of the M-alkyl bond induced by extended UV light exposure times, as has been previously reported by Alt and Rausch, and that may account for low intensity ^{1}H NMR spectroscopic signals that appear upon extended irradiation times.[38]

Encouraged by this preliminary data, we then determined the viability of PAGs as latent precatalyst activators for olefin polymerization, wherein 1-hexene was chosen for our initial studies so as to facilitate rapid screening without the need for complex glassware and gaseous monomer handling. 1-Hexene polymerizations were conducted using precatalyst **1** and 1 equiv. of PAG (Table 1, entries 1-2) using the irradiation conditions determined through the above described ^{1}H NMR spectroscopy studies (exposure time = 15 min, λ = 254 nm). Photoactivated polymerizations using precatalyst **1** with **I-PAG** produced 64% polymer yield (M_w = 19.7 kg/mol and $Đ$ = 2.6) (Table 1, entry 1), while polymerizations using **S-PAG** as a latent cocatalyst produced 40% polymer yield (M_w = 21.0 kg/mol, $Đ$ = 1.55) (Table 1, entry 2). These polymerizations were then compared to analogous polymerizations conducted using the traditional Brønsted acid activator **AB** (Table 1, entry 3). Both photoactivated systems using either **I-PAG** or **S-PAG** produced similar polymer molecular weights to polymerizations activated using **AB** (M_w = 19.7 - 25.3 kg/mol) (Table 1, entries 1-3). However, while polymerizations using **I-PAG** resulted in a comparable polymer yield to that of chemical activation with **AB** (64% versus 61% yield, respectively), polymerizations using **S-PAG** reproducibly resulted in lower polymer yields (40%), which we hypothesize may be due to the decreased solubility of **S-PAG** under the polymerization conditions used, the potential of sulfur byproducts to interfere with the active catalyst species, or a combination of these potentially contributing factors.

Though the results presented in Table 1 (entries 1 - 2) suggest that PIOP is possible, a series of control experiments were performed to validate the efficacy of PAGs as latent activators for olefin polymerization. First, it has been reported that UV light may induce homolytic cleavage of M-alkyl bonds within certain transition-metal species,[38] and therefore it must be confirmed that UV irradiation of precatalyst **1** alone (no PAG present) does not initiate olefin polymerization through any undesirable reactions, such as oxidation or reduction of the metal center. Indeed, no polymer is formed when precatalyst **1** is irradiated under the polymerization conditions employed (Table 1, entry 4). While this result does not exclude the possibility of homolytic cleavage of M-alkyl bonds upon UV irradiation, it does confirm that such events do not lead to olefin polymerization active species. Second, it is necessary to ensure that any products produced upon irradiation of either **I-PAG** or **S-PAG** do not initiate olefin polymerization in the absence of a precatalyst species. Once again, no polymer was produced from these control experiments (Table 1, entries 5 - 6) confirming that PAG photolysis alone does not lead to olefin polymerization active species. Lastly, we demonstrated that the combination of precatalyst **1**, **I-PAG** or **S-PAG**, dichloromethane, and 1-hexene in the absence of light does not result in any recoverable polymer (Table 1, entries 6-7), confirming that light irradiation is required for precatalyst activation and inadvertent precatalyst activation does not occur upon simple mixing of reagents. Based upon these control experiments, our results strongly support our initial hypothesis that PIOP using PAGs as latent precatalyst activators is a viable methodology for the synthesis of polyolefins.

Having demonstrated successful PIOP using PAGs as latent and light responsive olefin polymerization precatalyst activators, we sought to investigate how the ratio of PAG to precatalyst impacts 1-hexene polymerization. Using the polymerization conditions established above (10 μmol of precatalyst **1**, 3 mL of 1-hexene, 1 mL of dichloromethane, and 15 min of 254 nm light exposure), 1-hexene polymerizations were conducted as a function of PAG loading (0.5 -1.5 equiv) relative to that of precatalyst (Figure 2). Polymerizations using varying equivalents of **I-PAG** produced poly(1-hexene) yields ranging from 24 - 64%, whereas polymerizations using **S-PAG** produced poly(1-hexene) yields of 23 - 40%. In each case, it was found that a ratio of 1:1 (PAG:precatalyst) provided optimal polymer yield (64 ± 2.3% when using **I-PAG** and 40 ± 6.1% when using **S-PAG**) and consistent molecular weights (18.9 ± 0.9 kg/mol when using **I-PAG** and 19.0 ± 1.7 kg/mol when using **S-PAG**).

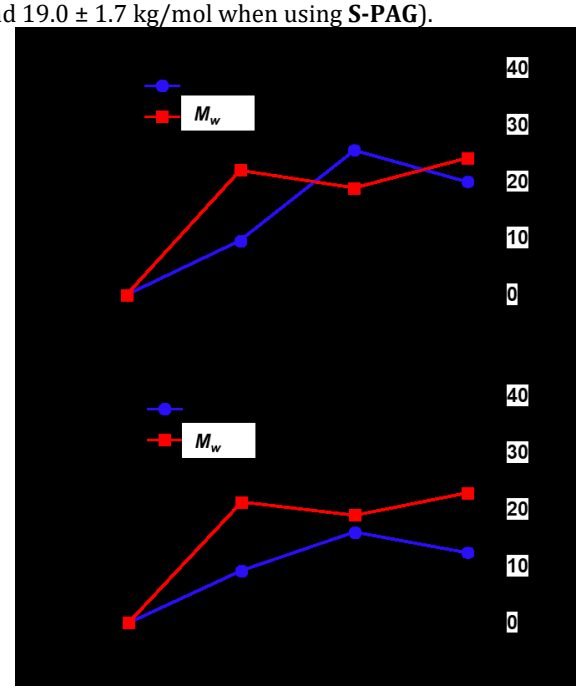

Figure 2. Plots of poly(1-hexene) yield and M_w as a function of a) **I-PAG** to precatalyst **1** ratio, and b) **S-PAG** to precatalyst **1** ratio.

The data presented in Figures 2a and 2b reveal that consistent molecular weight poly(1-hexene) was obtained at [**I-PAG**]/[**1**] or [**S-PAG**]/[**1**] ratios of 0.5, 1, or 1.5. This suggests that activated catalyst **1** may participate in either chain transfer or chain termination reactions that ultimately limit molecular weight. However, this observation is consistent with polymerizations ran using the traditional activator **AB** (Table 1, entry 3). We also suspect that the decreased polymer yields obtained when using excess **I-PAG** or **S-PAG** may result due to the in-situ generation of superstoichiometric photoacid, potentially leading to polyolefin protonolysis or deleterious catalyst deactivation. Furthermore, the decreased poly(1-hexene) yields produced when using an equimolar ratio (1:1) of **S-PAG** to precatalyst **1**, as compared to those obtained using **I-PAG**, may be due to **the** potential coordination of sulfur-containing biproducts, or **S-PAG**'s marginal solubility in the reaction solvents used.

The impact that UV exposure time has on PIOP efficiency was also investigated (Figure 3). Therein, poly(1-hexene) yield increased as a function of irradiation time up to 15 min of UV light exposure time when using either **I-PAG** (6 - 64%) and **S-PAG** (0 - 40%), which agrees well with ^{1}H NMR spectroscopy experiments described in Figure S3 in which optimal precatalyst activation occurs at ~15 min of irradiation time. In contrast, UV irradiation times extending up to 30 min resulted slight decreases in polymer yield.[38] Interestingly, PIOP using either **I-PAG** or **S-PAG** produced poly(1-hexene) with relatively consistent molecular weights of M_w = 18.6 - 26.0 kg/mol, and broad dispersity ($Đ$ = 1.47 - 2.77) regardless of exposure time, which is not unexpected given the chain-growth polymerization behavior of these catalysts. Ultimately, polymerizations employing precatalyst **1** and **I-PAG** proved to generate higher poly(1-hexene) yields, as compared to analogous polymerizations using **S-PAG**, under optimized PAG:precatalyst loadings and UV exposure times described above. Because of **I-PAG's** superior performance under the reaction conditions employed, the remainder of this study focuses exclusively on PIOP using **I-PAG**.

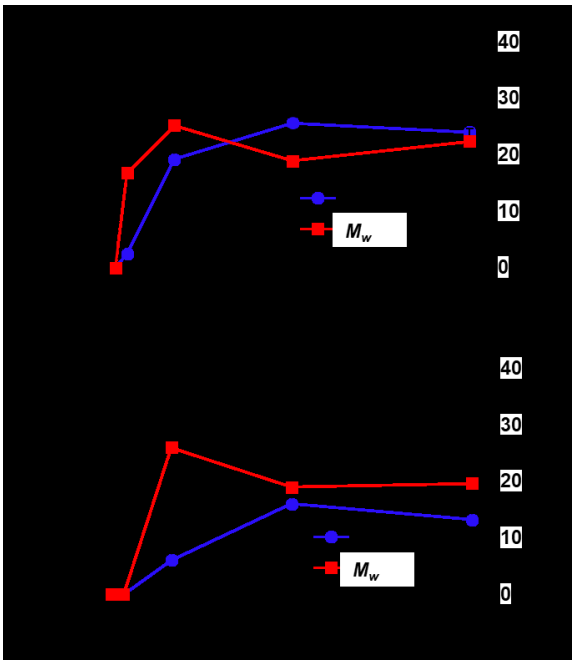

Figure 3. a) poly(1-hexene) yield as a function of irradiation time (**I-PAG** to precatalyst **1** ratio = 1:1), b) poly(1-hexene) yield as a function of irradiation time (**S-PAG** to precatalyst **1** ratio = 1:1).

As previously noted, the photoactivation of **1** with **I-PAG** resulted in a poly(1-hexene) yield similar to that of chemical activation using **AB**. In contrast, when photoactivating the Hf-based precatalyst **2** with **I-PAG**, a polymer yield of 43 ± 3.1% was obtain, which is more than double the polymer yield when using chemical activation (17 ± 0.1%), as seen in Figure 4a. While photoactivation of **2** with **I-PAG** resulted in an increase in polymer yield, the M_w (1.7 ± 0.1 kg/mol) was significantly lower than when activated using **AB** (5.0 ± 1.0 kg/mol). PIOP using the ONNO-type Zr-based precatalyst **3**, which is routinely activated via protonolysis using **AB**,[39-41] under 15 min of irradiation lead to slightly higher polymer yield (49 ± 4.0%) as compared to analogous polymerizations using the traditional activator **AB** (41 ± 0.9%). It should be noted that irradiation time longer than 15 min resulted in a significant decrease in polymer yield (9% at 30 min irradiation), as can be seen in Figure S11. We believe this decrease in yield at extended irradiation time is a result of photoinduced catalyst degradation.

Analysis of the poly(1-hexene) produced from the activation of precatalysts **1** - **3** using **I-PAG** revealed that photoactivation of precatalyst **1** and **2** produced mostly atactic polymer while activation of precatalyst **3** resulted in isotactic poly(1-hexene) analogous to the activation of **3** with **AB** (Figure S17).[41] Therefore, these results indicate that the tacticity of poly(α-olefins) resulting from precatalyst photoactivation using PIOP mimic those obtained using the traditional activator AB, and suggest that similar relationships between single-site catalyst symmetry elements and resultant tacticity hold when using PIOP.

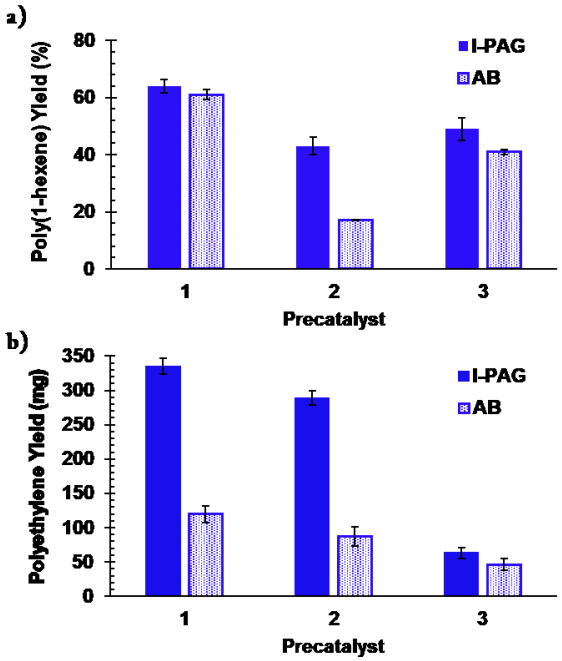

Figure 4. Plots of a) poly(1-hexene) yield from PIOP using precatalysts **1-3** as compared to results obtained using the traditional Brønsted acidic activator **AB**, and b) polyethylene yield from PIOP using precatalysts **1-3** as compared to results obtained using the traditional Brønsted acidic activator **AB**. All results obtained using an **I-PAG**:precatalyst ratio or **AB**:precatalyst ratio of 1:1).

We then extended our investigations to include the more industrially relevant feedstock, ethylene, which is a gaseous monomer at standard temperature and pressure (STP). Therein, ethylene polymerizations were conducted using precatalysts **1 - 3** using the optimized conditions established above, as well as their corresponding control experiments (Figure 4b). Similar to the results obtained for 1-hexene polymerization, precatalysts **1 - 3** produced a greater polymer yield when activated using PIOP and **I-PAG** than those activated with the traditional activator **AB**. Despite the observed differences in yield, the polyethylene samples produced using precatalysts **1-3** and PIOP displayed comparable molecular weights (M_w = 18.2 – 164.2) and dispersities ($Đ$ = 2.36 – 5.53) to those produced using **AB** (Table S2). Furthermore, Mark-Houwink plots of polyethylene intrinsic viscosity versus molecular weight for polymers produced using PIOP and **AB** virtually overlap one another, thereby suggesting that identical branching is observed regardless of the activation method chosen (see Figures S18-S19 for precatalysts **1** and **2**, respectively). Finally, control experiments similar to the ones described above (Table S2) once again confirmed that UV exposure is essential to facilitate PIOP using precatalysts **1 - 3** for ethylene polymerization, and that no unwanted polymerization occurs in the absence of light.

To determine if spatial control could be realized via the use of heterogeneous polymerizations (i.e. no solvent or liquid monomers present during polymerization) and gas-phase ethylene, solutions of desired precatalyst (**1 - 3**) and **I-PAG** were first prepared in DCM and shielded from ambient light. The precatalyst/**I-PAG** solution was then deposited onto a support substrate via drop-casting. The casting solvent quickly evaporated leaving a catalyst-activator residue on the substrate surface, which was loaded into a quartz pressure reactor (Figure S10). The reactor was pressurized with ethylene gas (30 psi) and irradiated using the same handheld 4 W compact UV lamp (254 nm) as used for the previous solution-state polymerizations. As anticipated, conformal polyethylene films were readily produced on both flat substrates as well as over those with varying topology. As an example, conformal films could be grown from objects such as a U.S. quarter by deposition of 5 mL of a 0.01 M solution containing precatalyst **2** and **I-PAG** in a 1:1 mole ratio. The polyethylene films obtained consistently ranged from 15 - 20 μm in thickness, and retained the quarter's surface topology in the free-standing polyethylene film when lifted off the surface by submerging in methanol.

The polyethylene films produced using heterogeneous PIOP of gaseous ethylene monomer were analyzed using size exclusion chromatography (Table S3). Precatalysts **1 - 3** each produced polyethylene films with broad dispersity ($Đ$ = 2.01-5.42) and notably high molecular weights (M_w = 604 -2,100 kg/mol), which were one order of magnitude higher than the polyethylene molecular weights produced via solution-state polymerizations. However, it should be noted that it is not uncommon for heterogeneous polymerizations to reach higher molecular weights as compared to analogous homogenous polymerizations.[42, 43] While PIOP using **3** and **I-PAG** produced a thin PE film, the mass of the film was insufficient for GPC analysis. Lastly, we found that heterogeneous PIOP could be employed to generate multi-layer structures via redeposition on previously grown polyethylene films. For example, a polyethylene film was grown from a 25 x 75 x 1 mm glass substrate through the deposition of 50 μmol of precatalyst **2** and **I-PAG** dissolved in 5 mL of dichloromethane. After producing the first polyethylene layer, a subsequent **2**/**I-PAG** layer was deposited, and a second polymer layer was grown upon UV light exposure under a gaseous ethylene feed. Film thickness was measured using a micrometer, and in a specific example, the layer thicknesses were found to be 26 ± 9 and 19 ± 4 μm for the first and second layers, respectively (46 ± 7 μm total thickness of both layers).

Thus far, we have demonstrated the ability to temporarily control the initiation of the polymerization of ethylene and 1-hexene through homogenous and heterogeneous polymerization. To further test our initial hypothesis, we investigated the ability of PIOP to achieved spatial control. This control over the olefin polymerization process using PIOP was demonstrated by deposition of a precatalyst **2**/**I-PAG** solution onto a glass slide and solvent evaporation. The precatalyst treated glass substrate was then covered with a photomask, which in this case was a square mask covered with aluminum tape (Figure 5a), followed by irradiation using UV light (254 nm) under a gaseous ethylene feed pressure. The photomask allowed a defined portion of the substrate to be irradiated while all other areas remain unexposed and is evidenced by the color changes from colorless to pink or yellow/orange as the irradiated **I-PAG** activates either precatalysts **1** or **2**, respectively, initiating olefin polymerization (Figures 5b-c). Submerging these films in a nonsolvent (methanol) quenches any remaining catalyst and the patterned

polyethylene films could then be lifted from the substrate. Scanning electron microscopy (SEM) of both exposed and unexposed regions conclusively confirm polymer film formation only in the areas defined by the photomask opening (Figure 5d) and demonstrate that heterogeneous PIOP can indeed provide spatial control over the olefin polymerization process.

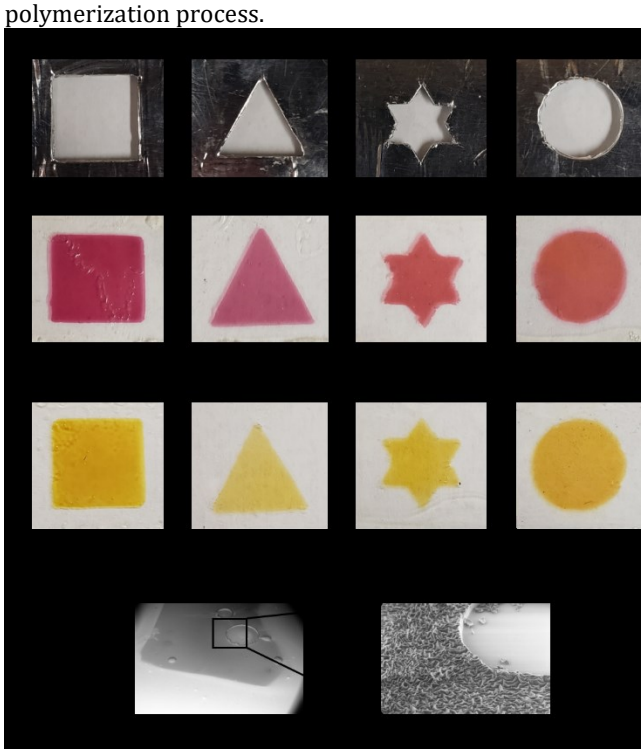

Figure 5. Demonstration of photopatterning and spatial resolution with heterogeneous PIOP using gaseous ethylene monomer (50 μmol precatalyst, 50 μmol **I-PAG**, 5 mL dichloromethane for casting, ethylene pressure = 30 psi, irradiation time = 15 min, total polymerization time = 30 min). Images are of a) photomasks used to demonstrate spatial control, b) patterned films produced using precatalyst **1** and **I-PAG**, c) patterned films produced using precatalyst **2** and **I-PAG**, and d) SEM images of a spatially patterned polyethylene film.

Conclusion

In sum, this report demonstrates that PAGs and UV light can be harnessed to activate of a variety of dialkyl-substituted olefin polymerization precatalysts, thereby initiating olefin polymerization (PIOP). We demonstrated that PIOP can provide control over the precise time of the catalyst activation process for solution-state polymerizations of ethylene and α-olefin monomers. Detailed ^{1}H NMR spectroscopic analysis suggests that UV exposure generates acidic protons through PAG photolysis that activate olefin polymerization precatalysts via protonolysis of metal-alkyl bonds to generate the cationic, active transition metal complexes required for polymerization. Following homogeneous, solution-state polymerization studies, we then demonstrated that PIOP is a viable method for the heterogeneous olefin polymerization of gaseous ethylene and propylene feedstocks. This heterogeneous polymerization strategy was used to produce conformal and layered polyolefin films. Finally, we confirmed that PIOP enables the ability to spatially control the olefin polymerization process in the absence of solvent. We believe that these fundamental results provide seminal evidence that PIOP may be of intertest for next-generation digital manufacturing methods, such as 3D printing processes that use gaseous olefin feedstocks to print polymeric structures using the world's most widely produced and versatile polymer class.

ASSOCIATED CONTENT

Supporting Information. Materials and methods, homogeneous and heterogeneous polymerization procedures, NMR spectra, additional tabulated polymerization data, UV-Vis spectra, and gel permeation chromatograms. This material is available free of charge via the Internet at http://pubs.acs.org.

AUTHOR INFORMATION

Corresponding Author

*Correspondence to: long@utk.edu

Author Contributions

‡These authors contributed equally

ACKNOWLEDGMENT

We would like to thank the NSF for providing financial support of this project under Award# 2203977. We thank 3D Systems, Inc. for their generous gift of **I-PAG** and **S-PAG**. We also thank Dr. Dayton Street and Dr. S. Michael Kilbey for creating the photomasks used for the heterogeneous photopolymerizations.

ABBREVIATIONS

PIOP, photoinduced initiation of olefin polymerization; PAG, photoacid generator; **AB**, anilinium tetrakis(pentafluorophenyl)borate; **I-PAG**,4-isopropyl-4'-methyldiphenyliodonium tetrakis(pentafluoro-phenyl)borate; **S-PAG**, bis[4-(dimethylphenylsulfonio)phenyl]-sulfonium tetrakis(pentafluorophenyl) borate.

REFERENCES

1. Geyer, R.; Jambeck, J. R.; Law, K. L., Production, use, and fate of all plastics ever made. *Sci. Adv.* **2017,** *3* (7), e1700782.
2. Coates, G. W.; Hustad, P. D.; Reinartz, S., Catalysts for the Living Insertion Polymerization of Alkenes: Access to New Polyolefin Architectures Using Ziegler–Natta Chemistry. *Angew. Chem. Int. Ed.* **2002,** *41* (13), 2236-2257.
3. Domski, G. J.; Rose, J. M.; Coates, G. W.; Bolig, A. D.; Brookhart, M., Living alkene polymerization: New methods for the precision synthesis of polyolefins. *Prog. Polym. Sci.* **2007,** *32* (1), 30-92.
4. Coates, G. W., Precise Control of Polyolefin Stereochemistry Using Single-Site Metal Catalysts. *Chem. Rev.* **2000,** *100* (4), 1223-1252.
5. Zhang, Y., Keaton, R. J., Sita, L. R., Degenerative Transfer Living Ziegler-Natta Polymerization: Application to the Synthesis of Monomodal Stereoblock Polyolefins of Narrow Polydispersity and Tunable Block Length. *J. Am. Chem. Soc.* **2003,** *125*, 9062-9069.
6. Harney, M. B.; Zhang, Y.; Sita, L. R., Discrete, multiblock isotactic-atactic stereoblock polypropene

microstructures of differing block architectures through programmable stereomodulated living Ziegler-Natta polymerization. *Angew. Chem. Int. Ed. Engl.* **2006,** *45* (15), 2400-4.
7. Jayaratne, K. C., Sita, L.R., Stereospecific Living Ziegler−Natta Polymerization of 1-Hexene. *J. Am. Chem. Soc.* **2000,** *122*, 958-959.
8. Koterwas, L. A., Fettinger, J. C., Sita L.R., Stereospecific Syntheses, Metal Configurational Stabilities, and Conformational Analyses of meso-(R,S)- and (R,R)-(eta5-C5R5)Ti(CH3)2-N,N'-bis(1-phenylethyl)acetamidinates for R = H and Me. *Organometallics* **1999,** *18*, 4183-4190.
9. Yan, T.; Guironnet, D., Combination of olefin insertion polymerization and olefin metathesis to extend the topology and composition of polyolefins. *Sci. China Chem.* **2020,** *63* (6), 755-757.
10. Walsh, D. J.; Hyatt, M. G.; Miller, S. A.; Guironnet, D., Recent Trends in Catalytic Polymerizations. *ACS Catal.* **2019,** *9* (12), 11153-11188.
11. Liu, Q.; Jordan, R. F., Multinuclear Palladium Olefin Polymerization Catalysts Based on Self-Assembled Zinc Phosphonate Cages. *Organometallics* **2018,** *37* (24), 4664-4674.
12. Zhai, F.; Jordan, R. F., (α-Diimine)nickel Complexes That Contain Menthyl Substituents: Synthesis, Conformational Behavior, and Olefin Polymerization Catalysis. *Organometallics* **2017,** *36* (15), 2784-2799.
13. Chen, E. Y.-X.; Marks, T. J., Cocatalysts for Metal-Catalyzed Olefin Polymerization: Activators, Activation Processes, and Structure−Activity Relationships. *Chem. Rev.* **2000,** *100* (4), 1391-1434.
14. Leibfarth, F. A.; Mattson, K. M.; Fors, B. P.; Collins, H. A.; Hawker, C. J., External regulation of controlled polymerizations. *Angew. Chem. Int. Ed. Engl.* **2013,** *52* (1), 199-210.
15. Doerr, A. M.; Burroughs, J. M.; Gitter, S. R.; Yang, X.; Boydston, A. J.; Long, B. K., Advances in Polymerizations Modulated by External Stimuli. *ACS Catal.* **2020,** *10* (24), 14457-14515.
16. Kuznetsova, N. A.; Malkov, G. V.; Gribov, B. G., Photoacid generators. Application and current state of development. *Russ. Chem. Rev.* **2020,** *89* (2), 173-190.
17. Shirai, M.; Tsunooka, M., Photoacid and photobase generators: Chemistry and applications to polymeric materials. *Prog. Polym. Sci.* **1996,** *21* (1), 1-45.
18. Woods, E. F.; Berl, A. J.; Kantt, L. P.; Eckdahl, C. T.; Wasielewski, M. R.; Haines, B. E.; Kalow, J. A., Light Directs Monomer Coordination in Catalyst-Free Grignard Photopolymerization. *J. Am. Chem. Soc.* **2021,** *143* (44), 18755-18765.
19. Barsoum, D. N.; Kirinda, V. C.; Kang, B.; Kalow, J. A., Remote-Controlled Exchange Rates by Photoswitchable Internal Catalysis of Dynamic Covalent Bonds. *J. Am. Chem. Soc.* **2022,** *144* (23), 10168-10173.
20. Michaudel, Q.; Kottisch, V.; Fors, B. P., Cationic Polymerization: From Photoinitiation to Photocontrol. *Angew. Chem. Int. Ed. Engl.* **2017,** *56* (33), 9670-9679.
21. Fors, B. P.; Hawker, C. J., Control of a Living Radical Polymerization of Methacrylates by Light. *Angew. Chem. Int. Ed.* **2012,** *51* (35), 8850-8853.
22. Trotta, J. T.; Fors, B. P., Organic Catalysts for Photocontrolled Polymerizations. *Synlett* **2016,** *27* (05), 702-713.
23. Ma, Y.; Kottisch, V.; McLoughlin, E. A.; Rouse, Z. W.; Supej, M. J.; Baker, S. P.; Fors, B. P., Photoswitching Cationic and Radical Polymerizations: Spatiotemporal Control of Thermoset Properties. *J. Am. Chem. Soc.* **2021,** *143* (50), 21200-21205.
24. Keyes, A.; Basbug Alhan, H. E.; Ha, U.; Liu, Y.-S.; Smith, S. K.; Teets, T. S.; Beezer, D. B.; Harth, E., Light as a Catalytic Switch for Block Copolymer Architectures: Metal–Organic Insertion/Light Initiated Radical (MILRad) Polymerization. *Macromolecules* **2018,** *51* (18), 7224-7232.
25. Dau, H.; Keyes, A.; Basbug Alhan, H. E.; Ordonez, E.; Tsogtgerel, E.; Gies, A. P.; Auyeung, E.; Zhou, Z.; Maity, A.; Das, A.; Powers, D. C.; Beezer, D. B.; Harth, E., Dual Polymerization Pathway for Polyolefin-Polar Block Copolymer Synthesis via MILRad: Mechanism and Scope. *J. Am. Chem. Soc.* **2020,** *142* (51), 21469-21483.
26. Kaiser, J. M.; Anderson, W. C.; Long, B. K., Photochemical regulation of a redox-active olefin polymerization catalyst: controlling polyethylene microstructure with visible light. *Polym. Chem.* **2018,** *9* (13), 1567-1570.
27. Khalimon, A. Y.; Leitao, E. M.; Piers, W. E., Photogeneration of a Phosphonium Alkylidene Olefin Metathesis Catalyst. *Organometallics* **2012,** *31* (15), 5634-5637.
28. Keitz, B. K.; Grubbs, R. H., A Tandem Approach to Photoactivated Olefin Metathesis: Combining a Photoacid Generator with an Acid Activated Catalyst. *J. Am. Chem. Soc.* **2009,** *131* (6), 2038-2039.
29. Li, R.; Nakashima, T.; Kawai, T., A self-contained photoacid generator for super acid based on photochromic terarylene. *ChemComm* **2017,** *53* (31), 4339-4341.
30. Klikovits, N.; Knaack, P.; Bomze, D.; Krossing, I.; Liska, R., Novel photoacid generators for cationic photopolymerization. *Polym. Chem.* **2017,** *8* (30), 4414-4421.
31. Chen, M.; Zhong, M.; Johnson, J. A., Light-Controlled Radical Polymerization: Mechanisms, Methods, and Applications. *Chem. Rev.* **2016,** *116* (17), 10167-211.
32. Devi, R.; Murugavel, S. C., Synthesis, spectral, and thermal characterization of photoreactive epoxy resin containing cycloalkanone moiety in the main chain. *J. Appl. Polym. Sci.* **2012,** *124* (1), 58-66.
33. Barzan, C.; Mino, L.; Morra, E.; Groppo, E.; Chiesa, M.; Spoto, G., Photoinduced Ethylene Polymerization on Titania Nanoparticles. *ChemCatChem* **2017,** *9* (23), 4324-4327.
34. Mino, L.; Barzan, C.; Martino, G. A.; Piovano, A.; Spoto, G.; Zecchina, A.; Groppo, E., Photoinduced Ethylene Polymerization on the CrVI/SiO2 Phillips Catalyst. *J. Phys. Chem C.* **2019,** *123* (13), 8145-8152.
35. Shi, S.; Croutxé-Barghorn, C.; Allonas, X., Photoinitiating systems for cationic photopolymerization: Ongoing push toward long wavelengths and low light intensities. *Prog. Polym. Sci.* **2017,** *65*, 1-41.
36. Cipullo, R.; Busico, V.; Fraldi, N.; Pellecchia, R.; Talarico, G., Improving the Behavior of Bis(phenoxyamine) Group 4 Metal Catalysts for Controlled Alkene Polymerization. *Macromolecules* **2009,** *42* (12), 3869-3872.

37. Moscato, B. M.; Zhu, B.; Landis, C. R., Mechanistic Investigations into the Behavior of a Labeled

Zirconocene Polymerization Catalyst. *Organometallics* **2012,** *31*, 2097−2107.
38. Alt, H.; Rausch, M. D., Photochemical reactions of dimethyl derivatives of titanocene, zirconocene, and hafnocene. *J. Am. Chem. Soc.* **1974,** *96* (18), 5936-5937.
39. Busico, V.; Cipullo, R.; Pellecchia, R.; Ronca, S.; Roviello, G.; Talarico, G., Design of Stereoselective Ziegler-Natta Propene Polymerization Catalysts. *Proc. Natl. Acad. Sci. U. S. A.* **2006,** *103* (42), 15321-15326.
40. Busico, V.; Cipullo, R.; Friederichs, N.; Ronca, S.; Talarico, G.; Togrou, M.; Wang, B., Block Copolymers of Highly Isotactic Polypropylene via Controlled Ziegler−Natta Polymerization. *Macromolecules* **2004,** *37* (22), 8201-8203.
41. Tshuva, E. Y.; Goldberg, I.; Kol, M., Isospecific Living Polymerization of 1-Hexene by a Readily Available Nonmetallocene C2-Symmetrical Zirconium Catalyst. *J. Am. Chem. Soc.* **2000,** *122* (43), 10706-10707.
42. Xie, T.; McAuley, K. B.; Hsu, J. C. C.; Bacon, D. W., Gas Phase Ethylene Polymerization: Production Processes, Polymer Properties, and Reactor Modeling. *Ind. Eng. Chem. Res.* **1994,** *33* (3), 449-479.
43. Tannous, K.; Soares, J. B. P., Gas-phase polymerization of ethylene using supported metallocene catalysts: Study of polymerization conditions. *Macromol. Chem. Phys.* **2002,** *203* (13), 1895-1905.

Graphic entry for the Table of Contents (TOC).